3352 *Macromolecules* **2010**, *43*, 3352–3358
DOI: 10.1021/ma1001386

Macromolecules
ARTICLE

Ranking the Stability of Perfluorinated Membranes Used in Fuel Cells to Attack by Hydroxyl Radicals and the Effect of Ce(III): A Competitive Kinetics Approach Based on Spin Trapping ESR

Marek Danilczuk, Andrew J. Perkowski,† and Shulamith Schlick*

Department of Chemistry and Biochemistry, University of Detroit Mercy, 4001 West McNichols Road, Detroit, Michigan 48221. †NSF Research Experience for Undergraduate (REU) Fellow.

Received January 19, 2010; Revised Manuscript Received February 13, 2010

ABSTRACT: The stability of Nafion, stabilized Nafion (StNafion), and 3M and Aquivion membranes to attack by the hydroxyl radical, $HO^{\bullet}$, was compared in their aqueous dispersions at 300 K. $HO^{\bullet}$ radicals were generated by UV irradiation of hydrogen peroxide (H_2O_2), and radicals were detected by spin trapping with 5,5-dimethyl-1-pyrroline-*N*-oxide (DMPO). Two types of adducts were detected in all dispersions: DMPO/OH and DMPO/CCR, an adduct of carbon-centered radicals (CCRs) derived from the polymers. The competitive kinetics (CK) approach that has been adapted for ranking the polymer stability leads to the determination of their reaction rate constant with hydroxyl radicals. The experiments consisted of measuring the concentration of the DMPO/OH adduct in the presence of the polymers, which are considered to be "competitors" that react with $HO^{\bullet}$ radicals and compete with the spin trapping reaction $HO^{\bullet} + DMPO \rightarrow$ DMPO/OH. The results indicated an improved stability in StNafion compared with Nafion. The largest effect was, however, detected for the 3M and Aquivion polymers, which were significantly more stable. Examination of the hyperfine splittings of DMPO/CCR and of published reports suggests that the absence of the ether group and of the tertiary carbon in the side chain appears to be responsible for the greater stability of these ionomers. The addition of Ce(III) to the polymer dispersions led to a lower total concentration of the adducts DMPO/OH and DMPO/CCR. This result provided evidence for scavenging of $HO^{\bullet}$ radicals by Ce(III) that also leads to a lower concentration of the DMPO/CCR adduct. The CK approach was used to determine the reaction rate constant of Ce(III) with the $HO^{\bullet}$ radicals: $k_{Ce} = 2.8 \times 10^8\ M^{-1}\ s^{-1}$, in good agreement with the literature value of $3 \times 10^8\ M^{-1}\ s^{-1}$. The present experiments reaffirmed the centrality of $HO^{\bullet}$ radicals as an aggressive oxygen species involved in membrane degradation, the important effect of the side chain structure on membrane stability, and the stabilizing presence of Ce(III).

Introduction

Ionomeric membranes perform a central role in the operation of fuel cells: by separating the anode and cathode sections, by allowing hydrogen cations to diffuse from the anode to the cathode, and by blocking the flow of reduced oxygen species from the cathode to the anode.[1] The "traffic light" role of these proton exchange membranes (PEMs) is efficient when the integrity of the membrane molecular structure is maintained under the strongly oxidizing conditions of a fuel cell (FC). Whereas perfluorinated ionomers such as Nafion have held center stage in the operation of FCs, sulfonated hydrocarbon membranes have recently become valid alternatives.[2]

The durability of PEMs is a much studied topic in the current literature, and the major goals are to determine the nature of the attacking species and the site of attack.[3] Whereas initial studies on the degradation of perfluorinated membranes containing side chains terminated by sulfonic groups (PFSA) have concluded that the degradation mechanism is by the unzipping of the membrane backbone due to attack of hydroxyl radicals on end-chain $-COOH$ groups,[4,5] recent studies have provided evidence for the vulnerability of the Nafion side chain to degradation.[6,7]

Our studies have focused on early events in the degradation of PFSAs and model compounds by detection of the initially generated free radicals using direct electron spin resonance (ESR) and spin trapping ESR.[8−13] In an important development in our studies, we have studied the radical species in an FC inserted in the resonator of the ESR spectrometer and detected separately at the anode and at the cathode the presence of hydroxyl radicals ($HO^{\bullet}$), hydroperoxyl radicals ($HOO^{\bullet}$), hydrogen and deuterium atoms ($H^{\bullet}$ and $D^{\bullet}$), and carbon-centered radicals (CCRs) derived from Nafion.[14] These species were detected at 300 K by spin trapping with DMPO (Scheme 1). The capture of short-lived radicals by the diamagnetic spin trap leads to the formation of a paramagnetic spin adduct with higher stability: a nitroxide radical. In most cases, the identification of the trapped radical is based on simulating the experimental ESR spectra, determining the hyperfine splitting (hfs) from ^{14}N (a_N) and from Hβ protons ($a_{H\beta}$), and comparing the results with the literature, including the Spin Trapping Database.[15]

The centrality of hydroxyl radicals in the degradation mechanism of PFSAs was a major conclusion from our results: Hydrogen peroxide (H_2O_2) is formed in FCs in small concentrations but is not considered to be a main damaging agent. $HO^{\bullet}$ is the most reactive of the reactive oxygen species and in most cases the only attacking species.[16] This latter idea was a major conclusion of our recent study on the effect of Ce(III) as a neutralizing cation for a Nafion-based membrane-electrode assembly (MEA/Ce) in an FC inserted in the ESR resonater. The stabilizing effect of Ce(III) was clearly documented: in contrast with results of the study of the MEA/H FC,[14] no $HO^{\bullet}$ radicals and no membrane-derived CCRs were detected. We note that the DMPO/OOH was

*Corresponding author. Tel: 1-313-993-1012. Fax: 1-313-993-1144. E-mail: schlicks@udmercy.edu.

 Published on Web 02/19/2010

Scheme 1. Spin Trapping by 5,5-Dimethyl-1-pyrroline-*N*-oxide (DMPO)

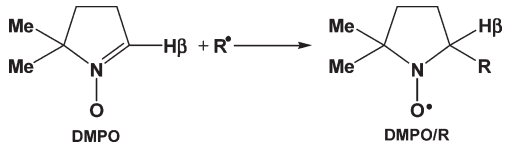

Chart 1. Nafion, 3M, and Aquivion Membranes

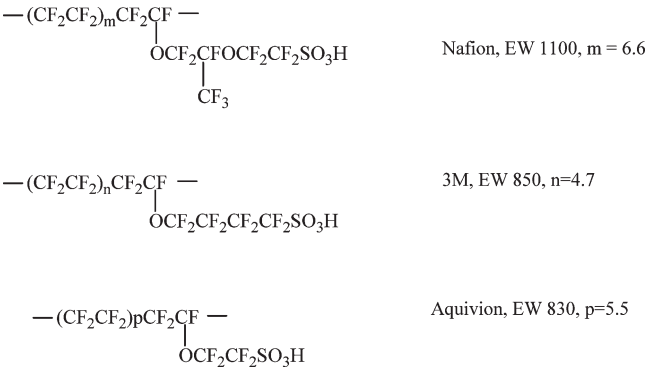

detected, thus proving that $HOO^{\bullet}$ is a less aggressive oxidant. Several recent studies have demonstrated that small amounts of Ce(III) and Mn(II) ions as well as metal oxides to the membrane can significantly reduce the rate of degradation.[17−20] Our study of the MEA/Ce FC has illuminated the in situ degradation mechanism of membrane stabilization by cationic additives.

In the present study, we focus on the effect of PFSA structure on the rate of reaction with $HO^{\bullet}$ radicals for Nafion, stabilized Nafion (StNafion), and 3M and Aquivion membranes as aqueous dispersions at 300 K. The hydroxyl radicals were generated by UV irradiation of H_2O_2, and the radicals were detected by spin trapping with DMPO. Nafion, 3M, and Aquivion membranes are shown in Chart 1. StNafion is a chemically stabilized Nafion, in which the concentration of −COOH end groups was reduced. The reactivity of the four membranes was compared by a kinetic approach based on the competition for $HO^{\bullet}$ radicals between the spin trap and the membrane. As described below, this study has evidenced the much higher stability of the 3M and Aquivion membranes compared with Nafion and StNafion.

Experimental Section

Materials. High purity DMPO from Alexis Biochemicals was used as received. Aqueous solutions of H_2O_2 (3%) were from Fisher Scientific. Methanol 99.8% and $CeCl_3$ were purchased from Sigma-Aldrich.

The Nafion dispersion (N117, 10 wt %) was also from Sigma-Aldrich. The stabilized Nafion aqueous dispersion (StNafion 117, D 1021, 10 wt %) was obtained from Ion Power, Inc. The 3M membrane aqueous dispersion (F12217, EW 825, 18 wt %) was from Steven Hamrock of 3M Co. The Aquivion dispersion (D83-20B, 20 wt %, EW 830) was supplied by Ajedium Films, Newark, DE (a division of Solvay-Solexis). Deionized "ultra pure" water with low conductivity and <10 ppb total organic carbon was obtained by the Millipore model Direct-Q UV system and used in the preparation of the solutions.

Sample Preparation. All experiments were performed in aqueous media. In a typical experiment, 1 mL of solution contained 8.8×10^{-5} M DMPO, 8.8×10^{-3} M H_2O_2, and the indicated amounts of Ce(III) (0 to 1 mM) or membrane (0−10 wt %). The pH of the solutions was adjusted with LiOH. Low pH values were avoided because of the low stability of nitroxides in highly acidic media.[21] All samples were prepared in quartz capillary tubes, placed inside the ESR resonator, and UV irradiated at 300 K in situ using the Oriel Xe-free UV source equipped with the UG-11 bandpass optical filter.

Electron Spin Resonance Measurements. These measurements were carried out at 300 K using a Bruker X-band EMX spectrometer operating at 9.7 GHz and 100 kHz magnetic field modulation and equipped with an ER 4105DR double rectangular resonator and ER 4111 VT variable temperature controller. The ESR spectra were simulated using the WinSim software package,[22] which also calculates the relative intensity of each spectral component when the ESR spectrum consists of a superposition of contributions from several spin adducts. Typical margin of error in the determination of relative intensities is about ±5%.

Competitive Kinetics (CK). The rate constant for the reaction between the perfluorinated ionomers and hydroxyl radicals was determined by measuring the intensity of the DMPO/OH adduct as a function of UV irradiation time first in the absence and then in the presence of the "competitor, C" whose reaction rate constant is determined. The major kinetic steps in the early stages of the reaction are

$$HO^{\bullet} + \mathrm{DMPO} \rightarrow \mathrm{DMPO/OH} \quad (\text{rate constant } k_{\mathrm{DMPO}}) \quad (1)$$

$$HO^{\bullet} + \mathrm{C} \rightarrow \mathrm{C}^{\bullet} \text{ or other products} \quad (\text{rate constant } k_{\mathrm{C}}) \quad (2)$$

Reaction 1 is the trapping of $HO^{\bullet}$ radicals by the spin trap, and reaction 2 is the inhibition of $HO^{\bullet}$ trapping reaction by the competitor C. $C^{\bullet}$ is the radical species that can be generated by the reaction of $HO^{\bullet}$ with the competitor. If we assume that the solution is saturated in the spin trap, then a simple kinetic analysis leads to eq 3, where V and v are, respectively, the rate of formation of the DMPO/OH adduct in the absence and in the presence of the competitor.[23−25]

$$\frac{V}{v} - 1 = \frac{k_{\mathrm{C}}[\mathrm{C}]}{k_{\mathrm{DMPO}}[\mathrm{DMPO}]} \quad (3)$$

The plot of $(V/v) - 1$ versus [C]/[DMPO] is expected to be linear, and the slope gives the ratio $k_{\mathrm{C}}/k_{\mathrm{DMPO}}$ and a measure of the ability of the competitor to react with hydroxyl radicals. The value of interest is k_{C}, which can be deduced from the slope of the above plot if the value of k_{DMPO} is known. As we will see below, we are interested in k_{M} for the membrane as competitor and k_{Ce} for Ce(III) as the competitor.

Control Experiments. Two types of experiments were performed.

(*a*). *Checking the Sensitivity of the Membrane Dispersions to UV Irradiation*. These experiments were performed in the presence of DMPO but in the absence of H_2O_2 and therefore also in the absence of hydroxyl radicals. No signals were detected in experiments with Nafion, StNafion, and Aquivion dispersions. In the case of 3M dispersions obtained from 3M in 2005 and 2007, a strong signal from a DMPO/CCR adduct was detected. Such signals were not detected for the 3M dispersion received in 2009, and all experiments with 3M dispersions reported in this study were performed with this non-UV-sensitive dispersion.

(*b*). *Verifying the Kinetic Approach*. The control experiment was the generation of the DMPO/OH adduct in the presence of methanol as a competitor, determination of k_{DMPO}, and comparison with literature values. Figure S1-A in the Supporting Information shows representative ESR spectra of the DMPO/OH adduct obtained after 30 s of UV irradiation at 300 K in the absence and in the presence of the indicated concentrations of methanol. In the absence of methanol, only the DMPO/OH adduct, with $a_{\mathrm{N}} = a_{\mathrm{H}} = 14.8$ G, was detected. In the presence of methanol, the additional signal of the DMPO/CH_2OH adduct, with $a_{\mathrm{N}} = 15.9$ G and $a_{\mathrm{H}} = 22.7$ G, appeared; these hfs are in good agreement with literature data.[24] The peak height of the second low field peak of the DMPO/OH adduct was monitored (red arrow in Figure SI-A in the Supporting Information).

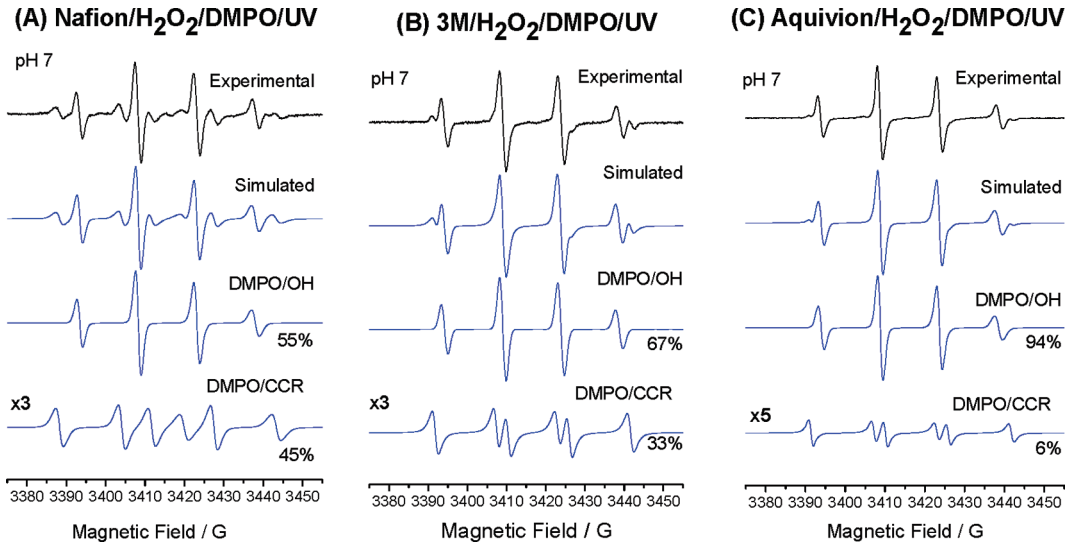

Figure 1. Experimental ESR spectra of DMPO adducts detected at 300 K in aqueous dispersions of Nafion, 3M, and Aquivion membranes containing 3% H_2O_2 and corresponding simulated spectra. UV irradiation times were 5 min for Nafion and 3M membranes and 60 min for the Aquivion membrane. The concentration of the ionomers in the dispersions was 10 wt %. CCR stands for a carbon-centered radical. The relative intensities of adducts are shown on the right. The simulations were performed with fixed $a_N = a_H = 14.8$ G for the DMPO/OH adduct in all systems; these values were read directly from the ESR spectra.

During the first 30 s of UV irradiation, the peak growth was linear. The relative intensity of the two adducts, DMPO/OH and DMPO/CH_2OH, varies with methanol content. The inhibition of the DMPO/OH adduct formation in the presence of different methanol concentrations is shown in Figure S1-B. The results are plotted in Figure S2 in the Supporting Information as the variation of $(V/v) - 1$ with the [MeOH/DMPO] ratio. Using $k_{MeOH} = 9.7 \times 10^8$ M^{-1} s^{-1} for the reaction between methanol and hydroxyl radicals,[26] the absolute rate constant for DMPO/OH adduct formation (reaction 1 above) was calculated: $k_{DMPO} = 3.6 \times 10^9$ M^{-1} s^{-1}. As seen in Table S1 in the Supporting Information, this value of k_{DMPO} is in excellent agreement with literature data, thus providing the appropriate confidence in our approach. We note that the literature values are in the range of (2.7 to 4.3) $\times 10^9$ M^{-1} s^{-1}.

Results and Discussion

1. DMPO/OH and DMPO/CCR Adducts in the Ionomer Dispersions. The ESR spectra detected in the Nafion, 3M, and Aquivion membrane dispersions exposed to hydroxyl radicals at pH 7 are shown in Figure 1A−C, respectively. The spectra were simulated in terms of two spectral components: DMPO/CCR and DMPO/OH. We noticed that the relative intensity of the adduct from the carbon-centered radical (CCR) is higher in the case of Nafion (45%, 5 min UV) compared with 3M (33%, 5 min UV) and much lower than both for Aquivion (6%, 1 h UV). Slightly different relative intensities were measured at pH 4.

Table 1 presents the hfs of the DMPO/OH and DMPO/CCR adducts. The data suggest that the attack of hydroxyl radicals leads to two types of radicals: (1) The values of a_N and a_H for the 3M and Aquivion membranes are identical, suggesting that the same type of radical was generated and trapped. For these ionomers, the magnetic parameters of the DMPO/CCR adduct are identical to those detected in UV-irradiated sodium formate, $NaHCO_2$, and identified as the DMPO adduct of carbon dioxide radical anion, $CO_2^{\bullet -}$, with $a_N = 15.7$ G and $a_H = 18.7$ G.[27] We therefore propose that the presence of the CCR in 3M and Aquivion systems indicates attack of $HO^\bullet$ radicals on the carboxylic end groups of the ionomer backbone. We note that an identical DMPO/CCR was also detected in our study of CF_2HCOOH as a model compound but was not identified at that time.[13] Taken together, it appears that we identified, for first time, an adduct generated by attack of $HO^\bullet$ radicals on the −COOH end groups and confirmed the unzipping mechanism. (2) For Nafion and StNafion, the parameters for the adduct are $a_N = 15.9$ G and $a_H = 23.5$. We suggest that, in contrast with 3M and Aquivion systems, the radicals generated in Nafion and StNafion are a result of the attack of hydroxyl radicals on the side chains.

Table 1. Magnetic Parameters of DMPO Adducts in the Ionomer Dispersions

membrane	adduct	a_N/G	a_H/G
Nafion 10 wt % 1100EW Sigma-Aldrich	DMPO/CCR	15.9	23.4
	DMPO/OH	14.8	14.8
StNafion 10 wt % 1100EW DE1021 IonPower Inc.	DMPO/CCR	16.2	23.5
	DMPO/OH	14.8	14.8
3M 10 wt % 825EW F12217 3M	DMPO/CCR	15.7	18.7
	DMPO/OH	14.8	14.8
Aquivion 10 wt % 830EW D83-20B Solvay Solexis	DMPO/CCR	15.7	18.7
	DMPO/OH	14.8	14.8

In principle, the determination of the relative intensity of the DMPO/CCR adducts in the four systems studied may provide a method to determine the relative stabilities of the ionomers. However, data on the percent of DMPO/CCR adducts depend on the simulation of the experimental ESR spectra and deconvolution into the relative intensities: an indirect method that can describe semiqualitative observations but is not totally dependable quantitatively. For this reason, we preferred to compare ionomer reactivities to attack of $HO^\bullet$ radicals by a more direct method: competitive kinetics (CK).

2. Competitive Kinetics: Perfluorinated Ionomers as Competitors For $HO^\bullet$ Radicals. We have adapted the CK approach to compare the reaction rates of the ionomers with hydroxyl radicals. The results are shown in Figures 2 and 3. The thick black line in Figure 2A shows the formation of hydroxyl radicals in the absence of Nafion. Data collected in

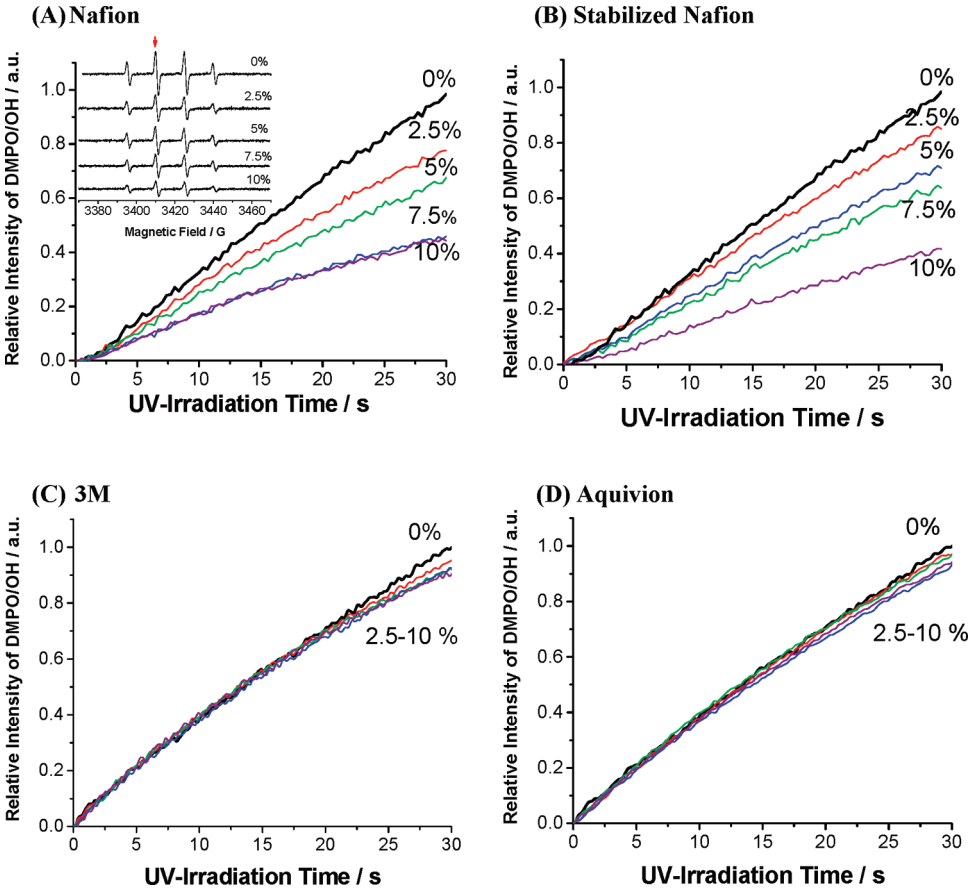

Figure 2. ESR spectra of the DMPO/OH adduct for the indicated Nafion concentrations in the range of 0−10 wt % are shown in the inset of (A); the red arrow indicates the peak that was monitored in the time scans. The intensity of the ESR signal from the DMPO/OH adduct as a function of polymer concentration is shown in the time scans: (A) Nafion, (B) StNafion, (C) 3M membrane, and (D) Aquivion. The thicker black line in each case shows the results in the absence of ionomers; data collected in the presence of ionomers were normalized to the intensity measured in the absence of each ionomer after 30 s of UV irradiation at 300 K.

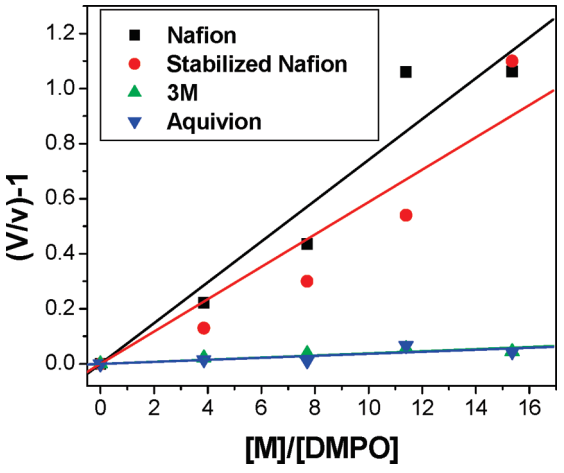

Figure 3. Plots of $(V/v) - 1$ versus the concentration ratio [M]/[DMPO] for Nafion (■), stabilized Nafion (●), 3M (▲), and Aquivion (▼) using the inhibition data of the DMPO/OH adduct shown in Figure 2. Note that the polymer membrane concentration, [M], is expressed in terms of the number of backbone carbons. Data for each system were fitted by assuming that the straight lines extrapolate to the origin.

the presence of Nafion were normalized to the intensity measured after 30 s of UV irradiation at 300 K in the absence of the ionomer; we notice the linear variation of adduct relative intensity and the progressively lower intensity detected in the time scans measured when the ionomer concentration increased. The inset in Figure 2A presents the ESR spectra of the DMPO/OH adduct in Nafion dispersions for increasing concentrations of the ionomer; the red arrow points to the height of the signal that was monitored in the time scans.

The results for StNafion, 3M, and Aquivion systems are presented in Figures 2B−D, respectively, as a function of irradiation time for the indicated ionomer concentrations, whereas the signal shown by the red arrow in the inset of Figure 2A was monitored. The addition of both Nafion and StNafion significantly inhibits the formation of DMPO/OH spin adduct. The effect of 3M and Aquivion ionomers is, however, negligible; these results suggest a greater stability of these ionomers under the experimental conditions used in our laboratory.

In Figure 3, we present the analysis of the results shown in Figure 2 by CK: plots of $(V/v) - 1$ as a function of the concentration ratios [M]/[DMPO], where the concentration of the polymeric membranes in the dispersions is expressed as the number of backbone carbons. The degradation mechanism is complicated and involves both the unzipping of the main chain through −COOH chain ends[3−6] and the attack of hydroxyl radicals on the side chain.[6,7,9,11,12,28] Expressing [M] in terms of the backbone atoms is somewhat arbitrary but will allow a comparison of membrane reactivity.

The corresponding slopes in Figure 3 are the values of k_M/k_{DMPO}; k_M, the reaction rate constant for the reaction of the ionomer with hydroxyl radicals, was determined by multiplying the slope by k_{DMPO}. The results are shown in Table 2.

Table 2. Reaction Rates of Fluorinated Ionomers with Hydroxyl Radicals[a]

membrane	k_M/k_{DMPO}	$k_M/M^{-1}\ s^{-1}$
Nafion	0.0741	2.7×10^8
StNafion	0.0588	2.1×10^8
3M	0.0038	0.14×10^8
Aquivion	0.0037	0.13×10^8

[a] k_M values are calculated for [M] expressed as the number of carbons in main chain.

The k_M values shown in Table 2 clearly indicate the stability of 3M and Aquivion ionomers to attack by hydroxyl radicals and the slightly greater stability of StNafion compared with Nafion.

We caution, however, that the ranking of membranes in terms of their stability is based on the polymer concentration expressed arbitrarily in terms of the number of backbone carbons. Therefore, the k_M values listed in Table 2 should be considered for comparison only.

It is important to understand the greater stability of 3M and Aquivion membranes compared with both Nafion and StNafion. The major difference between the two groups of membranes is the structure of the side chain, as seen in Chart 1. Search of the recent literature illuminates the subtle effects of structure on the degradation mechanism. In our study of a model compound (MC) that mimicked the Nafion side chain, $CF_3CF_2OCF_2CF_2SO_3H$ (perfluoro-(2-ethoxyethane) sulfonic acid, PFEESA), we have detected adducts of both CCRs and oxygen-centered radicals with DMPO and 2-methyl-2-nitrosopropane (MNP) used as the spin traps;[13] these adducts suggested the cleavage of the C−O bond when exposed to the hydroxyl radicals generated by UV irradiation of H_2O_2. Zhou et al. described a study of MCs exposed to Fenton conditions;[6] for the MCs that contained ether groups but no terminal −COOH groups, the major conclusion was that the ether linkages can lead to side-chain cleavage. Chen and Fuller described the side-chain scission for Nafion in an FC environment and studied by FTIR the effect of the relative humidity;[28] the bands at 984 and 969 cm^{-1} were assigned to C−O−C groups from the polymer backbone and from the side chain, respectively. Moreover, the presence of trifluoroacetic acid (TFA) was traced to the decomposition of the ether group in the side chain. These studies[6,13,28] provided strong evidence for the susceptibility of the ether group in the side chain to attack by hydroxyl radicals, based on both ex situ studies in the laboratory and in situ studies in a FC.

The major structural difference among the polymers studied is the absence of the ether group and of the tertiary carbon in the side chain of the 3M and Aquivion membranes. The results presented in this study suggest that this structural variation is responsible for the greater stability of these membranes, as visualized in Figure 3 and Table 2. Additional support for these conclusions can be seen in Table 1. The hfs of the DMPO/CCR adducts for the 3M and Aquivion systems suggest the generation of a radical by attack of hydroxyl radicals on the −COOH end groups; the side chain was not attacked. Consideration of the results for the MCs as well as the in situ data discussed above encouraged us to propose that the radical in Nafion and in StNafion was generated by the attack of hydroxyl radicals on the side chain. In this stage, we are seeking additional confirmation of these conclusions by a comparative FTIR study of all four membranes.[29]

The vulnerability of the ether group in the side chain may be greater in the ionomer dispersions compared with the dry membranes because the side chains are exposed to water and ions, whereas the main chain backbone is assembled into bundles of elongated aggregates.[30−32] In the membranes, especially at low relative humidity, the side chains are expected to be less accessible to hydroxyl radicals and therefore less prone to cleavage.

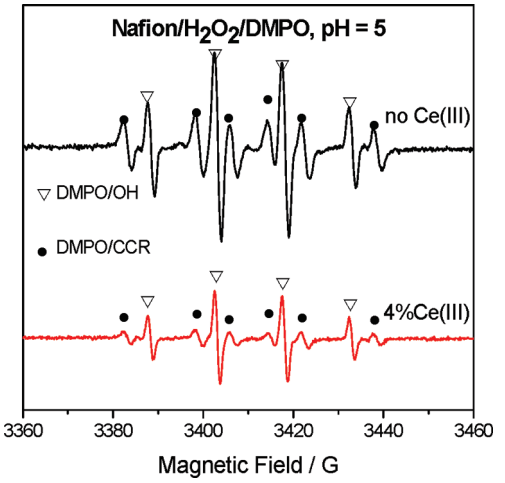

Figure 4. Effect of Ce(III) on the intensity of the DMPO/CCR adduct in Nafion dispersions exposed to hydroxyl radicals. Top spectrum: no Ce(III). Bottom spectrum: For the ionomer that was 4% neutralized by Ce(III). Triangles and circles show the signals from the DMPO/OH and DMPO/CCR adducts, respectively.

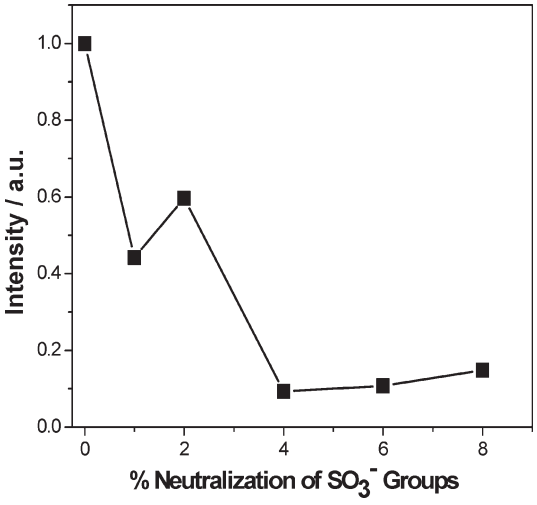

Figure 5. Intensity of the DMPO/CCR adduct in Nafion dispersions as a function of the degree of neutralization by Ce(III).

3. Ce(III) as Competitor. Figure 4 shows the ESR spectra of DMPO/OH and DMPO/CCR for Nafion dispersions at pH 5 in the absence (top) and in the presence of Ce(III) (bottom). The ratio of the relative intensities of the two adducts is about the same in both spectra: [DMPO/OH]/[DMPO/CCR] is 70/30 ± 1. The absolute intensity of the adducts is, however, greatly reduced in the presence of Ce(III): the sum of integrated intensities of both DMPO adducts in the presence of Ce(III) is lower by a factor of ~12. These results clearly indicate that Ce(III) is a scavenger for hydroxyl radicals, as is also documented in our recent in situ study of a FC based on MEA/Ce, a Nafion membrane 10% neutralized by Ce(III).[16] Because the hydroxyl radical concentration is lower in the presence of Ce(III), the concentration of the $HO^{\bullet}$-generated DMPO/CCR adduct is also lower.

A full picture of the Ce(III) effect is shown in Figure 5: A decrease by approximately a factor of 10 of the DMPO/CCR adduct concentration is detected when 4% of the sulfonic

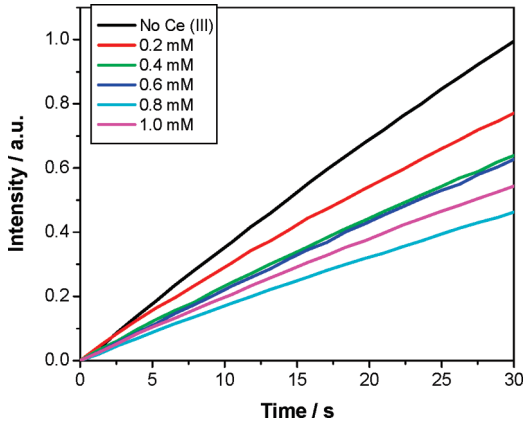

Figure 6. Ce(III) as a competitor for hydroxyl radicals: Inhibition of DMPO/OH adduct formation by the indicated concentration of Ce(III) ions in water solution during UV irradiation at 300 K.

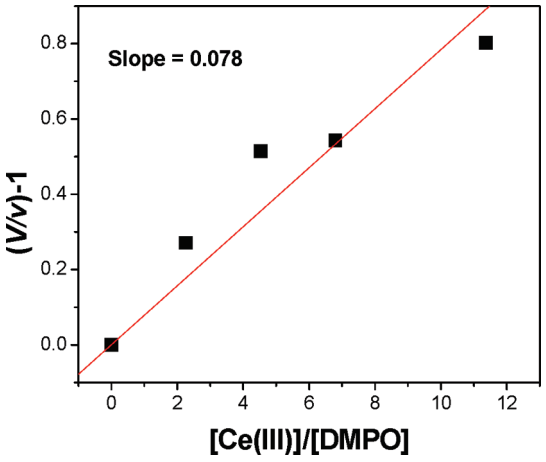

Figure 7. Plot of $(I/v) - 1$ versus the [Ce(III)]/[DMPO] ratio. The value of $k_{Ce} = 2.8 \times 10^8$ M^{-1} s^{-1} was determined by multiplying the slope, k_{Ce}/k_{DMPO}, by $k_{DMPO} = 3.6 \times 10^9$ M^{-1} s^{-1}. See the text.

groups were neutralized by Ce(III), as is also shown in Figure 4, indicating that Ce(III) is a strong competitor for hydroxyl radicals. It was assumed, of course, that one Ce(III) ion neutralizes three $-SO_3^-$ groups.

The inhibition of DMPO/OH formation is presented in Figure 6 as a function of time for the indicated Ce(III) concentrations, and the corresponding CK plot is in Figure 7. From these experiments, we have determined $k_{Ce} = 2.8 \times 10^8$ M^{-1} s^{-1}, which is in excellent agreement with literature value of 3×10^8 M^{-1} s^{-1}.[26] Because the concentration of Ce(III) is well-defined, this value of k_{Ce} can be considered to be an absolute value.

The ranking of membrane stability to attack by $HO^\bullet$ radicals and the stabilizing effect of Ce(III) described above suggest that we are poised to define both the delicate and essential role of membrane structure on the degradation process as well as the method and mechanism of membrane stabilization by select additives.

Conclusions

The stability of Nafion, stabilized Nafion (StNafion), 3M, and Aquivion ionomers to attack by hydroxyl radicals, $HO^\bullet$, was compared at 300 K. The $HO^\bullet$ radicals were generated in the aqueous ionomer dispersions by UV-irradiation of H_2O_2, and radical detection was achieved by spin trapping with 5,5-dimethyl-1-pyrroline-*N*-oxide (DMPO). Two types of adducts were detected in all dispersions: DMPO/OH and DMPO/CCR, an adduct of the CCRs derived from the ionomers. The CK approach that has been adapted for ranking the membrane stability leads to the determination of the reaction rate constant between hydroxyl radicals and the ionomers, k_M. The experiments consisted of measuring the concentration of the DMPO/OH adduct in the presence of the ionomers, which are considered to be "competitors" for the spin trapping reaction $HO^\bullet$ + DMPO.

The results indicated an improved stability in StNafion compared with Nafion. The largest effect was detected, however, for the 3M and Aquivion membranes, which were found to be significantly more stable than Nafion and StNafion by a factor of ~20. The absence of the ether group and of the tertiary carbon in the side chain appears to be responsible for the greater stability of these membranes. The hfs's of the DMPO/CCR adducts for the 3M and Aquivion systems suggest the generation of a radical by attack of $HO^\bullet$ radicals on the carboxylic end groups: the side chain was not attacked. Consideration of the results for the MCs as well as for in situ data encouraged us to propose that the radical in Nafion and in StNafion was generated by attack of hydroxyl radicals on the side chain.

Addition of Ce(III) to the polymer dispersions led to a lower concentration of both the DMPO/OH adduct and of DMPO/CCR, the adduct of the CCRs; for 4% neutralization of the sulfonic groups, the total integrated intensity of both adducts was lower by a factor of ~12 compared with the cerium-less solution. This result provided evidence of scavenging of $HO^\bullet$ radicals by Ce(III) and thus of a lower concentration of DMPO/CCR as well. The Ce(III) experiments reaffirmed the centrality of $HO^\bullet$ radicals as the most aggressive oxygen species involved in the membrane degradation process; this conclusion is in agreement with recent results deduced in a FC inserted in the ESR resonator, ref 16.

The CK approach was also used in this study to determine the reaction rate constant of Ce(III) with $HO^\bullet$ radicals; $k_{Ce} = 2.8 \times 10^8$ M^{-1} s^{-1}, in excellent agreement with literature value of 3×10^8 M^{-1} s^{-1}.

Acknowledgment. This research was supported by the U.S. Department of Energy Cooperative Agreement no. DE-FG36-07GO17006 and by the NSF (Polymers Program). DOE support does not constitute an endorsement by DOE of the views expressed in this presentation. We are grateful to Dr. Steven Hamrock of 3M Co. for numerous helpful discussions and to the two reviewers for their constructive criticism.

Supporting Information Available: Figure S1A presents the ESR spectra at 300 K of DMPO adducts recorded after 30 s of UV irradiation in the absence (top) and in the presence of the indicated methanol concentrations. Figure S1B shows the time scans: the intensity of the DMPO/OH adduct as a function of time for the indicated methanol concentration. Figure S2 illustrates the determination of the k_{MeOH}/k_{DMPO} ratio using the data shown in Figure S1B. Table S1 lists the literature rate constants at 300 K for spin trapping of hydroxyl radicals with DMPO, and the value determined in the present study. This material is available free of charge via the Internet at http://pubs.acs.org.

References and Notes

(1) Roduner, E.; Schlick, S. Chapter 8. In *Advanced ESR Methods in Polymer Research*; Schlick, S., Ed.; Wiley: Hoboken, NJ, 2006; pp 197–228.
(2) (a) Higashihara, T.; Matsumoto, K.; Ueda, M. *Polymer* **2009**, *50*, 5341–5357. (b) Yoshimura, K.; Iwasaki, K. *Macromolecules* **2009**, *42*, 8943–8949, 9302–9306.
(3) Borup, R.; Meyers, J.; Pivovar, B.; Kim, Y. S.; Mukundan, R.; Garland, N.; Myers, D.; Wilson, M.; Garzon, F.; Wood, D.;

Zelenay, P.; More, K.; Stroh, K.; Zawodinski, T.; Boncella, J.; McGrath, J. E.; Inaba, M.; Miyatake, K.; Hori, M.; Ota, K.; Ogumi, Z.; Miyata, S.; Nishikate, A.; Siroma, Z.; Uchimoto, Y.; Yasuda, K.; Kimijima, K. I.; Iwashita, N. *Chem. Rev.* **2007**, *107*, 3904–3951.
(4) Curtin, D. E.; Lousenberg, R. D.; Henry, T. J.; Tangeman, P. C.; Tisack, M. E. *J. Power Sources* **2004**, *131*, 41–48.
(5) Healy, J.; Hayden, C.; Xie, T.; Olson, K.; Waldo, R.; Brundage, A.; Gasteiger, H.; Abbott, J. *Fuel Cells* **2005**, *5*, 302–308.
(6) Zhou, C.; Guerra, M. A.; Qiu, Z.-M.; Zawodzinski, T. A.; Schiraldi, D. A. *Macromolecules* **2007**, *40*, 8695–8707.
(7) Ghassemzadeh, L.; Marrony, M.; Barrera, R.; Kreuer, K. D.; Maier, J.; Müller, K. *J. Power Sources* **2009**, *186*, 334–338.
(8) Bosnjakovic, A.; Schlick, S. *J. Phys. Chem. B* **2004**, *108*, 4332–4337.
(9) Kadirov, M. K.; Bosnjakovic, A.; Schlick, S. *J. Phys. Chem. B* **2005**, *109*, 7664–7670.
(10) Bosnjakovic, A.; Schlick, S. *J. Phys. Chem. B* **2006**, *110*, 10720–10728.
(11) Lund, A.; Macomber, L.; Danilczuk, M.; Stevens, J.; Schlick, S. *J. Phys. Chem. B* **2007**, *111*, 9484–9491.
(12) Danilczuk, M.; Bosnjakovic, A.; Kadirov, M. K.; Schlick, S. *J. Power Sources* **2007**, *172*, 78–82.
(13) Danilczuk, M.; Coms, F. D.; Schlick, S. *Fuel Cells* **2008**, *8*, 436–452.
(14) Danilczuk, M.; Schlick, S.; Coms, F. D. *J. Phys. Chem. B* **2009**, *113*, 8031–8042.
(15) Spin Trapping Database. http://tools.niehs.nih.gov/stdb/index.cfm.
(16) Danilczuk, M.; Coms, F. D.; Schlick, S. *Macromolecules* **2009**, *42*, 8943–8949.
(17) Endoh, E. *ECS Trans.* **2008**, *16*, 1229–1240.
(18) Trogadas, P.; Parrondo, J.; Ramani, V. *Electrochem. Solid-State Lett.* **2008**, *11*, B113–B116.
(19) Coms, F. D.; Liu, H.; Owejan, J. E. *ECS Trans.* **2008**, *16*, 1735–1747.
(20) (a) Frey, M. H.; Hamrock, S. J.; Haugen, G. M.; Pham, P. T. Fuel Cell Membrane Electrode Assembly. U.S. Patent 7,572,534, **2009**. (b) Frey, M. H.; Pierpont, D. M.; Hamrock, S. J. High Durability Fuel Cell Components With Cerium Salt Additives. U.S. Patent Application US2007/009905.
(21) Gaffney, B. J. Chapter 5. In *Spin Labeling, Theory, and Applications*; Berliner, L. J., Ed.; Academic Press: New York, 1976; pp 183−238.
(22) The software WinSim can be accessed at: http://www.niehs.nih.gov/research/resources/software/tools/index.cfm.
(23) Finkelstein, E.; Rosen, G. M.; Rauckman, E. J. *J. Am. Chem. Soc.* **1980**, *102*, 4994–4999.
(24) (a) Madden, K. P.; Taniguchi, H. *J. Am. Chem. Soc.* **1991**, *113*, 5541–5547. (b) Madden, K. P.; Taniguchi, H. *J. Phys. Chem.* **1996**, *100*, 7511–7516. (c) Taniguchi, H.; Madden, K. P. *J. Am. Chem. Soc.* **1999**, *121*, 11875–11879.
(25) (a) Villamena, F. A.; Zweier, J. L. *J. Chem. Soc. Perkin Trans. 2* **2002**, 1340–1344. (b) Villamena, F. A.; Hadad, C. M.; Zweier, J. L. *J. Phys. Chem. A* **2003**, *107*, 4407–4414.
(26) Buxton, G. V.; Greenstock, C. L.; Helman, W. P.; Ross, A. B. *J. Phys. Chem. Ref. Data* **1988**, *17*, 513–886.
(27) Villamena, F. A.; Locigno, E. J.; Rockenbauer, A.; Hadad, C. M.; Zweier, J. L. *J. Phys. Chem. A* **2006**, *110*, 13253–13258.
(28) Chen, C.; Fuller, T. F. *Polym. Degrad. Stab.* **2009**, *94*, 1436–1447.
(29) Danilczuk, M.; Lin, L.; Schlick, S., work in progress.
(30) Szajdzinska-Pietek, E.; Schlick, S.; Plonka, A. *Langmuir* **1994**, *10*, 1101–1109.
(31) Rubatat, L.; Rollet, A. L.; Gebel, G.; Diat, O. *Macromolecules* **2002**, *35*, 4050–4055.
(32) van der Haijden, P. C.; Rubatat, L.; Diat, O. *Macromolecules* **2004**, *37*, 5327–5336.